

See discussions, stats, and author profiles for this publication at: <https://www.researchgate.net/publication/11884578>

# Influence of Hydroxyl Substitution on Benzyne Properties. Quantum Chemical Characterization of the Didehydrophenols

ARTICLE *in* JOURNAL OF THE AMERICAN CHEMICAL SOCIETY · MARCH 2001

Impact Factor: 12.11 · DOI: 10.1021/ja002250l · Source: PubMed

---

CITATIONS

52

---

READS

9

2 AUTHORS, INCLUDING:



**Christopher J Cramer**

University of Minnesota Twin Cities

**531** PUBLICATIONS **23,344** CITATIONS

SEE PROFILE

# Influence of Hydroxyl Substitution on Benzyne Properties. Quantum Chemical Characterization of the Didehydrophenols

William T. G. Johnson and Christopher J. Cramer\*

Contribution from the Department of Chemistry and Supercomputer Institute, University of Minnesota, Minneapolis, Minnesota 55455-0431

Received June 22, 2000. Revised Manuscript Received November 9, 2000

**Abstract:** Geometries and singlet–triplet splittings for the 10 geometrical isomers of didehydrophenol are characterized at a variety of levels of electronic structure theory. The influence of the hydroxyl group is primarily to increase/decrease the weight of zwitterionic singlet mesomers that place positive/negative charge adjacent to oxygen in valence bond descriptions of the arynes. For some of the *meta* isomers, this interaction stabilizes distortion in the direction of a bicyclic geometry. The net effect, relative to the unsubstituted benzyne, is to increase the singlet–triplet splittings in 2,3-, 2,6-, and 3,5-didehydrophenol and to decrease that splitting in 2,4- and 2,5-didehydrophenol (3,4-didehydrophenol is essentially unaffected). As shown for other arynes, the singlet–triplet splittings can also be accurately estimated by correlation with proton hyperfine coupling constants in antecedent monoradicals, these values being accessible from very economical calculations.

## Introduction

*o*-Benzyne is an experimentally and theoretically well-characterized reactive intermediate having substantial synthetic utility.<sup>1,2</sup> Although they are typically more difficult to access experimentally, interest in *m*- and *p*-benzyne isomers has been renewed in the past decade by the discovery that in situ generated *p*-benzynes are implicated as the reactive species responsible for the activity of the so-called enediyne class of antitumor antibiotics.<sup>3</sup> (Cycloaromatization of 3-ene-1,5-diynes to *p*-benzynes was demonstrated by Jones and Bergman<sup>4</sup> several years prior to isolation of the first enediyne antibiotic.)

A significant factor decreasing the clinical utility of enediyne (and related) antibiotics is that the phenomenon responsible for their activity, namely, hydrogen atom abstraction from DNA sugars by the *p*-benzyne diradical, manifests itself with very little selectivity. This aggressive reactivity has been ascribed to a small splitting between the singlet and triplet states of the relevant benzyne.<sup>5–7</sup> Since the singlet–triplet (S–T) splitting, and thereby the reactivity, is expected to be sensitive to aryl substituents, the effect of such substituents on the chemistry of enediynes and related antitumor agents has received considerable attention.<sup>8–13</sup>

Several key properties of the unsubstituted “parent” benzyne, including heats of formation, S–T splittings, electron affinities, and some vibrational frequencies, have been determined from gas-phase negative ion photoelectron spectroscopy.<sup>14</sup> Additional information regarding gas-phase reactivity of substituted benzyne has derived from mass spectral studies; for instance, Thoen and Kenttämää<sup>15,16</sup> have characterized the reactivity of a *m*-benzyne substituted with a positively charged substituent.

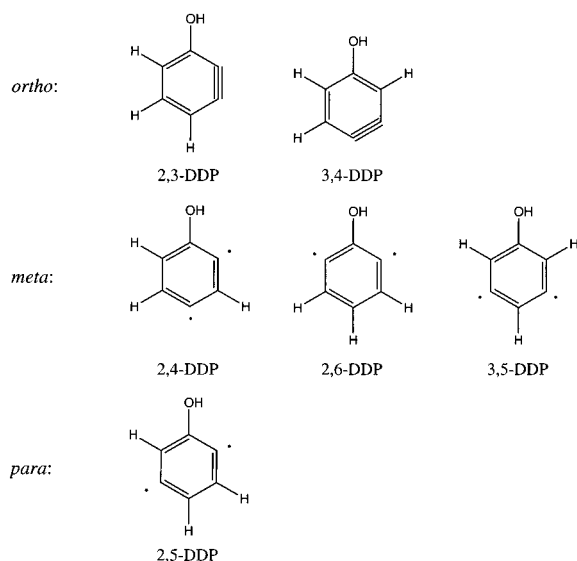
Additional data on the parent benzyne, particularly infrared spectra which have been useful in determining structure, have derived from matrix isolation spectroscopy.<sup>17,18</sup> The latter technique has moreover proved useful for the generation of substituted benzyne, including 2,4-didehydrophenol and some 6-alkyl-substituted analogues,<sup>19</sup> 3,5-didehydrofluorobenzene, and 3,5-didehydrotoluene.<sup>20</sup>

Theory has played a key role in characterizing the benzyne as well, to include substituted benzyne,<sup>20–25</sup> annelated benzyne,<sup>26–31</sup> and benzyne incorporating heteroatoms in the

- (1) Wentrup, C. *Reactive Molecules*; Wiley: New York, 1984; p 288.
- (2) Levin, R. H. In *Reactive Intermediates*; Jones, M., Moss, R., Eds.; Wiley: New York, 1985; Vol. 3, p 1.
- (3) *Enediyne Antibiotics as Antitumor Agents*; Borders, D. B., Doyle, T. W., Eds.; Marcel Dekker: New York, 1995.
- (4) Jones, R. R.; Bergman, R. G. *J. Am. Chem. Soc.* **1972**, *94*, 660.
- (5) Logan, C. F.; Chen, P. *J. Am. Chem. Soc.* **1996**, *118*, 2113.
- (6) Schottelius, M. J.; Chen, P. *J. Am. Chem. Soc.* **1996**, *118*, 4896.
- (7) Hoffner, J.; Schottelius, M. J.; Feichtinger, D.; Chen, P. *J. Am. Chem. Soc.* **1998**, *120*, 376.
- (8) Poon, R.; Beerman, T. A.; Goldberg, I. H. *Biochemistry* **1977**, *16*, 486.
- (9) Myers, A. G.; Kuo, E. Y.; Finney, N. S. *J. Am. Chem. Soc.* **1989**, *111*, 8057.
- (10) Nicolaou, K. C.; Dai, W.-M. *Angew. Chem., Int. Ed. Engl.* **1991**, *11*, 1387.
- (11) Myers, A. G.; Cohen, S. B.; Kwon, B.-M. *J. Am. Chem. Soc.* **1994**, *116*, 1670.
- (12) Myers, A. G.; Parrish, C. A. *Bioconj. Chem.* **1996**, *7*, 322.

- (13) Goldberg, I. H.; Kappen, L. S.; Xu, Y.-j.; Stassinopoulos, A.; Zeng, X.; Xi, Z.; Yang, C. F. In *DNA and RNA Cleavers and Chemotherapy of Cancer and Viral Diseases*; Meunier, B., Ed.; Kluwer: Amsterdam, 1996; p 1.
- (14) Wenthold, P. G.; Squires, R. R.; Lineberger, W. C. *J. Am. Chem. Soc.* **1998**, *120*, 5279.
- (15) Thoen, K. K.; Kenttämää, H. I. *J. Am. Chem. Soc.* **1997**, *119*, 3832.
- (16) Thoen, K. K.; Kenttämää, H. I. *J. Am. Chem. Soc.* **1999**, *121*, 800.
- (17) Chapman, O. L.; Mattes, K.; McIntosh, C. L.; Pacansky, J.; Calder, G. V.; Orr, G. *J. Am. Chem. Soc.* **1973**, *95*, 6134.
- (18) Sander, W. *Acc. Chem. Res.* **1999**, *32*, 669.
- (19) Sander, W.; Bucher, G.; Wandel, H.; Kraka, E.; Cremer, D.; Sheldrick, W. S. *J. Am. Chem. Soc.* **1997**, *119*, 10660.
- (20) Sander, W.; Exner, M. *J. Chem. Soc., Perkin Trans. 2* **1999**, 2285.
- (21) Bucher, G.; Sander, W.; Kraka, E.; Cremer, D. *Angew. Chem., Int. Ed. Engl.* **1992**, *35*, 746.
- (22) Marquardt, R.; Sander, W.; Kraka, E. *Angew. Chem., Int. Ed. Engl.* **1996**, *35*, 746.
- (23) Kraka, E.; Cremer, D.; Bucher, G.; Wandel, H.; Sander, W. *Chem. Phys. Lett.* **1997**, *268*, 313.
- (24) Davico, G. E.; Schwartz, R. L.; Ramond, T. M.; Lineberger, W. C. *J. Am. Chem. Soc.* **1999**, *121*, 6047.
- (25) Cramer, C. J. *J. Chem. Soc., Perkin Trans. 2* **1999**, 2273.
- (26) Ford, G. P.; Biel, E. R. *Tetrahedron Lett.* **1995**, *36*, 3663.
- (27) Cramer, C. J.; Squires, R. R. *J. Phys. Chem. A* **1997**, *101*, 9191.

Chart 1



aromatic ring.<sup>7,32–35</sup> This paper characterizes the 10 possible dihydroxyphenols (DDPs; six dihydro geometrical isomers, for four of which there are two distinct hydroxyl rotamers—see Chart 1) at levels of electronic structure theory that account for electron correlation in various ways. Chemically, we focus on the influence of the hydroxyl group on aryne geometries and singlet and triplet state energies. Comparison of all 10 isomers renders particularly clear the nature of certain influences. From a computational standpoint, we employ several different levels of electronic structure theory to ensure the validity of the chemical interpretations as well as to evaluate limitations in the application of certain theoretical levels to certain aryne isomers.

### Computational Methodology

Geometries were optimized at the multiconfigurational self-consistent-field (MCSCF) and density functional (DFT) levels of theory. In every case the correlation-consistent polarized valence-double- $\zeta$  basis set, cc-pVDZ,<sup>36</sup> was employed.

The MCSCF calculations were of the CASSCF variety.<sup>37</sup> For the arynes, eight electrons were included in the active space constructed from the six  $\pi$  orbitals of the aromatic ring and the two  $\sigma$  radical orbitals. This active space was reduced to seven electrons/orbitals for hydroxyphenyl radicals, and to six electrons/orbitals for phenol.

Two different DFT functionals were employed. Both used the gradient-corrected exchange functional of Becke,<sup>38</sup> which was combined either with the gradient-corrected correlation functional of Lee, Yang, and Parr<sup>39</sup> (BLYP) or that of Perdew et al.<sup>40</sup> (BPW91). Singlet aryne DFT “wave functions” that exhibited instability with respect to spin-symmetry breaking were optimized with unrestricted DFT. Vibrational

frequencies, zero-point vibrational energies, and thermal enthalpy contributions were calculated at the BLYP/cc-pVDZ level.

Dynamic electron correlation was also accounted for at the CASPT2 level<sup>41,42</sup> by using the MCSCF wave functions as reference. Some caution must be applied in interpreting the CASPT2 results since this level of theory is known to suffer from a systematic error proportional to the number of unpaired electrons.<sup>43</sup> CASPT2 energies were calculated for both MCSCF and DFT geometries. In addition, coupled-cluster calculations including single and double excitations and a perturbative estimate for triple excitations were carried out for single-configuration reference wave functions expressed in either Hartree–Fock (CCSD-(T)<sup>44,45</sup>) or Brueckner (BD(T)<sup>46</sup>) orbitals. Brueckner orbitals<sup>47</sup> eliminate contributions from single excitations in the coupled-cluster ansatz, and this can remove instabilities<sup>48</sup> associated with very large singles amplitudes in the more common CCSD(T) method. Such instabilities were manifest in the *p*-DDPs.

Analysis of CASPT2 and CCSD(T) (or BD(T)) energies for the MCSCF, BPW91, and BLYP geometries indicated that in every instance but one, the BLYP geometries were lower in energy (i.e., better). The sole exception was syn triplet 2,3-DDP, where the MCSCF geometry was predicted to be 1.1 kcal/mol lower at the CASPT2 level than the BLYP geometry. Thus, unless otherwise indicated, all data in this paper are computed with use of BLYP geometries. We note that Sander and Exner have also compared various functionals for their accuracy in predicting substituted *m*-benzyne geometries and concluded that the BLYP functional was optimal.<sup>20</sup> Similarly, Gräfenstein et al. have shown that the BLYP level of theory with a polarized double- $\zeta$  basis set compares well with experiment for a variety of unsubstituted aryne properties; they demonstrated that this agreement derives in part from a fortuitous cancellation of errors associated with basis set incompleteness and deficiencies in the functional.<sup>49</sup>

Partial atomic charges were computed by using Charge Model 2 at the BPW91/6-31G\* level of theory. BLYP/cc-pVDZ geometries were used; hydrogen charges are summed into the heavy atom to which the H is attached. Isotropic hyperfine coupling constants (hfs) were calculated as<sup>50</sup>

$$a_X = (4\pi/3)\langle S_z \rangle^{-1} g g_X \beta_X \rho(X) \quad (1)$$

where  $g$  is the electronic  $g$  factor,  $\beta$  is the Bohr magneton,  $g_X$  and  $\beta_X$  are the corresponding values for nucleus  $X$ , and  $\rho(X)$  is the Fermi contact integral

$$\rho(X) = \sum_{\mu\nu} P_{\mu\nu}^{\alpha-\beta} \phi_\mu(\mathbf{R}_X) \phi_\nu(\mathbf{R}_X) \quad (2)$$

where  $P^{\alpha-\beta}$  is the BPW91/cc-pVDZ one-electron spin density matrix, and evaluation of the overlap between basis functions  $\phi_\mu$  and  $\phi_\nu$  is only at the nuclear position,  $\mathbf{R}_X$ .

Multi- and single-reference calculations were carried out with the MOLCAS<sup>51</sup> and Gaussian 98<sup>52</sup> electronic structure program suites, respectively.

- (28) Schreiner, P. R. *J. Am. Chem. Soc.* **1998**, *120*, 4184.  
 (29) Squires, R. R.; Cramer, C. J. *J. Phys. Chem. A* **1998**, *102*, 9072.  
 (30) Schreiner, P. R. *Chem. Commun.* **1998**, 483.  
 (31) Koseki, S.; Fujimura, Y.; Hiram, M. *J. Phys. Chem. A* **1999**, *103*, 7672.  
 (32) Nam, H. H.; Leroi, G. E.; Harrison, J. F. *J. Phys. Chem.* **1991**, *95*, 6514.  
 (33) Cramer, C. J. *J. Am. Chem. Soc.* **1998**, *120*, 6261.  
 (34) Cramer, C. J.; Debbert, S. *Chem. Phys. Lett.* **1998**, *287*, 320.  
 (35) Debbert, S. L.; Cramer, C. J. *Int. J. Mass. Spectrom.* **2000**, *201*, 1.  
 (36) Dunning, T. H. *J. Chem. Phys.* **1989**, *90*, 1007.  
 (37) Roos, B. O.; Taylor, P. R.; Siegbahn, P. E. M. *Chem. Phys.* **1980**, *48*, 157.  
 (38) Becke, A. D. *Phys. Rev. A* **1988**, *38*, 3098.  
 (39) Lee, C.; Yang, W.; Parr, R. G. *Phys. Rev. B* **1988**, *37*, 785.  
 (40) Perdew, J. P.; Burke, K.; Wang, Y. *Phys. Rev. B* **1996**, *54*, 16533.

- (41) Andersson, K.; Malmqvist, P.-Å.; Roos, B. O.; Sadlej, A. J.; Wolinski, K. *J. Phys. Chem.* **1990**, *94*, 5483.  
 (42) Andersson, K. *Theor. Chim. Acta* **1995**, *91*, 31.  
 (43) Andersson, K.; Roos, B. O. *Int. J. Quantum Chem.* **1993**, *45*, 591.  
 (44) Purvis, G. D.; Bartlett, R. J. *J. Chem. Phys.* **1982**, *76*, 1910.  
 (45) Raghavachari, K.; Trucks, G. W.; Pople, J. A.; Head-Gordon, M. *Chem. Phys. Lett.* **1989**, *157*, 479.  
 (46) Handy, N.; Pople, J. A.; Head-Gordon, M.; Raghavachari, K.; Trucks, G. W. *Chem. Phys. Lett.* **1989**, *164*, 185.  
 (47) Brueckner, K. A. *Phys. Rev.* **1954**, *96*, 508.  
 (48) Stanton, J. F. *Chem. Phys. Lett.* **1997**, *281*, 130.  
 (49) Gräfenstein, J.; Cremer, D. *Phys. Chem. Chem. Phys.* **2000**, *2*, 2091.  
 (50) Lim, M. H.; Worthington, S. E.; Dulles, F. J.; Cramer, C. J. In *Density-Functional Methods in Chemistry*; Laird, B. B., Ross, R. B., Ziegler, T., Eds.; ACS Symp. Ser. No. 629; American Chemical Society: Washington, DC, 1996; p 402.  
 (51) Andersson, K.; Blomberg, M. R. A.; Fülscher, M. P.; Karlström, G.; Kellö, V.; Lindh, R.; Malmqvist, P.-Å.; Noga, J.; Olsen, J.; Roos, B. O.; Sadlej, A. J.; Siegbahn, P. E. M.; Urban, M.; Widmark, P.-O. *MOLCAS-3*; University of Lund: Sweden, 1994.

**Table 1.** Singlet DDP BSEs ( $H_{298}$ , kcal/mol)<sup>a</sup>

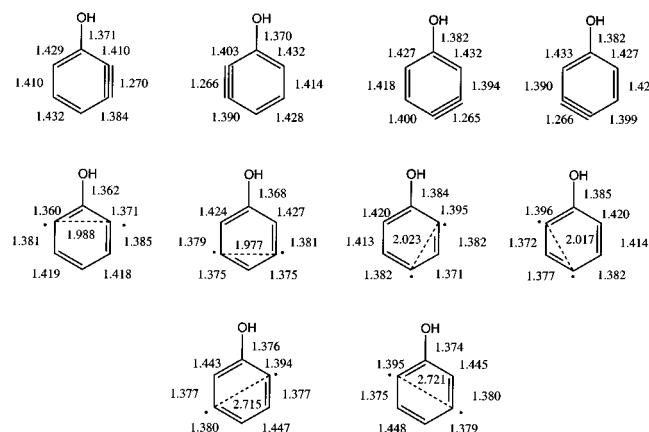
level	<i>ortho</i>				<i>meta</i>		<i>para</i>			
	<i>syn</i> -2,3	<i>anti</i> -2,3	<i>syn</i> -3,4	<i>anti</i> -3,4	2,6	3,5	<i>syn</i> -2,4	<i>anti</i> -2,4	<i>syn</i> -2,5 <sup>b</sup>	<i>anti</i> -2,5 <sup>b</sup>
BLYP	−38.3	−38.6	−34.4	−34.1	−26.4	−23.5	−18.6	−18.0	−3.1	−3.1
CASPT2	−37.6	−38.0	−34.6	−34.4	−25.5	−22.8	−18.4	−17.9	−2.7	−2.6
CCSD(T)	−37.4	−37.8	−34.5	−34.1	−25.6	−22.8	−18.5	−17.9	−2.8 <sup>c</sup>	−3.1 <sup>c</sup>

<sup>a</sup> All calculations used the cc-pVDZ basis set and BLYP optimized geometries; see eqs 3 and 4 for BSE definition. <sup>b</sup> Geometry optimized with unrestricted (broken spin symmetry) BLYP. <sup>c</sup> BD(T).

**Table 2.** Triplet DDP BSEs ( $H_{298}$ , kcal/mol)<sup>a</sup>

level	<i>ortho</i>				<i>meta</i>				<i>para</i>	
	<i>syn</i> -2,3	<i>anti</i> -2,3	<i>syn</i> -3,4	<i>anti</i> -3,4	2,6	3,5	<i>syn</i> -2,4	<i>anti</i> -2,4	<i>syn</i> -2,5	<i>anti</i> -2,5
BLYP	2.3	3.2	1.7	1.5	1.6	1.3	−0.2	−0.1	−1.1	−1.1
CASPT2	4.4	3.3	1.8	1.7	1.4	1.1	−0.1	0.0	−0.9	−1.0
CCSD(T)	4.3	3.7	2.1	1.9	1.6	1.3	0.0	0.1	−1.0 <sup>b</sup>	−1.0 <sup>b</sup>

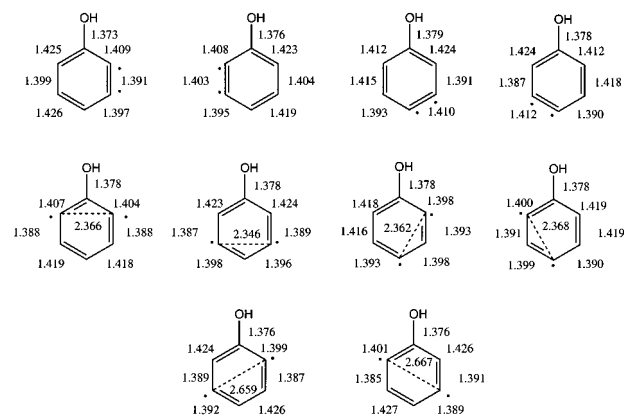
<sup>a</sup> All calculations used the cc-pVDZ basis set and BLYP optimized geometries; see eqs 3 and 4 for BSE definition. <sup>b</sup> BD(T).

**Figure 1.** Heavy atom bond lengths (Å) for singlet DDPs at the BLYP/cc-pVDZ level. In every case, the O–H bond is oriented in-plane to the right.

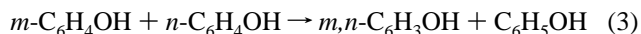
## Results and Discussion

Heavy atom bond distances for the singlet and triplet DDPs are presented in Figures 1 and 2, respectively. While we analyze individual isomers in more detail below, we note here that there is a general trend for C–C bonds to a dehydro center to be shortened and C–C bonds one bond further away (i.e., anti-periplanar to the nonbonding orbital) to be lengthened relative to the unperturbed aromatic system. The effects oppose one another for some bonds in the *o*- and *m*-DDPs while the bond-lengthening effect is reinforcing in the *p*-DDPs, which show some of the longest antiperiplanar C–C bonds. The source of the shortening effect is simply enhanced *s* character in the contribution of the dehydro carbon to the  $\sigma$  bonding orbital, while the source of the lengthening effect is hyperconjugation between the parallel C–C  $\sigma$  bonding and  $\sigma^*$  antibonding orbitals and the nonbonding orbital at the dehydro position.<sup>53</sup> Whether the C–C  $\sigma$  orbital acts as a donor or the  $\sigma^*$  orbital acts as an acceptor, the net effect is to decrease the bond order.

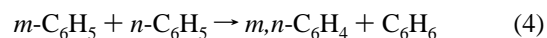
Biradical stabilization energies (BSEs) for the singlet and triplet DDPs are presented in Tables 1 and 2, respectively. To

**Figure 2.** Heavy atom bond lengths (Å) for triplet DDPs at the BLYP/cc-pVDZ level. In every case, the O–H bond is oriented in-plane to the right.

maximize chemical accuracy, BSE is defined in this paper by a multistep process. First, we compute the 298 K heat of reaction for the isodesmic process



where *m* and *n* represent dehydro positions. Thus, eq 3 measures the enthalpy change associated with interaction of the two dehydro positions in DDP compared to the monoradicals. The BSE values from eq 3 are then corrected for each level of theory by the amount necessary to make that level agree with experiment<sup>14,54</sup> for the BSE of the corresponding benzyne, defined as the 298 K heat of reaction for



This correction scheme largely eliminates any idiosyncratic behavior exhibited by particular levels of theory for particular isomers, so that the span of predicted BSEs in Tables 1 and 2 is quite small—typically less than 0.5 kcal/mol. Figure 3 plots the CCSD(T) (or BD(T)) BSEs for all isomers to facilitate identification of chemical trends.

The difference in BSEs for the singlet and triplet spin states defines the 298 K singlet–triplet (S–T) splitting. Experimentally, such splittings are more typically reported as 0 K quantities

(54) The experimental BSEs ( $H_{298}$ , kcal/mol) are  $-35.6 \pm 3.6$ ,  $-20.6 \pm 3.6$ , and  $-4.2 \pm 2.1$  for singlet *o*-, *m*-, and *p*-benzyne, respectively, and  $2.1 \pm 3.6$ ,  $0.8 \pm 2.8$ , and  $-0.4 \pm 2.2$  for the triplet states, respectively. The experimental S–T splittings ( $H_0$ , kcal/mol) are  $-37.5 \pm 0.3$ ,  $-21.0 \pm 0.3$ , and  $-3.8 \pm 0.5$ , respectively.

(52) Frisch, M. J.; Trucks, G. W.; Schlegel, H. B.; Gill, P. M. W.; Johnson, B. G.; Robb, M. A.; Cheeseman, J. R.; Keith, T. A.; Petersson, G. A.; Montgomery, J. A.; Raghavachari, K.; Al-Laham, M. A.; Zakrzewski, V. G.; Ortiz, J. V.; Foresman, J. B.; Peng, C. Y.; Ayala, P. A.; Wong, M. W.; Andres, J. L.; Replogle, E. S.; Gomperts, R.; Martin, R. L.; Fox, D. J.; Binkley, J. S.; Defrees, D. J.; Baker, J.; Stewart, J. P.; Head-Gordon, M.; Gonzalez, C.; Pople, J. A. *Gaussian 98*; Gaussian, Inc.: Pittsburgh, PA, 1998.

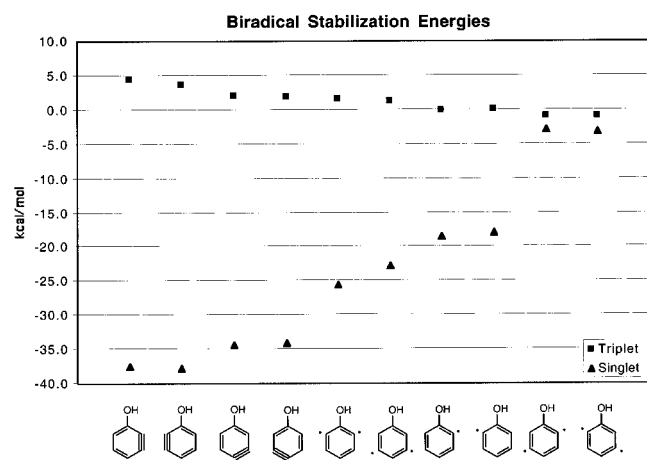
(53) Hoffmann, R.; Imamura, A.; Hehre, W. J. *J. Am. Chem. Soc.* **1968**, *90*, 1499.



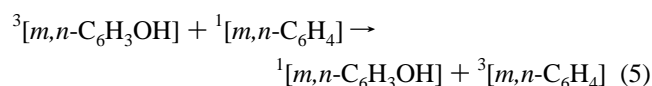
**Table 3.** DDP S–T Splittings ( $H_0$ , kcal/mol)<sup>a</sup>

level	<i>ortho</i>				<i>meta</i>				<i>para</i>	
	<i>syn</i> -2,3	<i>anti</i> -2,3	<i>syn</i> -3,4	<i>anti</i> -3,4	2,6	3,5	<i>syn</i> -2,4	<i>anti</i> -2,4	<i>syn</i> -2,5 <sup>b</sup>	<i>anti</i> -2,5 <sup>b</sup>
BLYP <sup>c</sup>	−40.4	−41.4	−35.9	−35.4	−28.0	−24.9	−18.5	−18.1	−2.1	−2.0
CASPT2 <sup>c</sup>	−41.8	−41.0	−36.2	−35.8	−26.8	−24.0	−18.5	−18.1	−1.8	−1.6
CCSD(T) <sup>c</sup>	−41.9	−41.1	−36.2	−35.8	−27.1	−24.2	−18.6	−18.2	−1.9 <sup>d</sup>	−2.2 <sup>d</sup>
from hfs <sup>e</sup>	−40.2	−41.5	−36.9	−36.4	−26.4	−23.3	−19.3	−19.6	−2.0	−2.2

<sup>a</sup> All calculations used the cc-pVDZ basis set. BLYP optimized geometries unless otherwise indicated. <sup>b</sup> Singlet geometry optimized with unrestricted (broken spin symmetry) BLYP. <sup>c</sup> See eqs 3–5 and discussion in text. <sup>d</sup> BD(T). <sup>e</sup> BPW91 geometries; see text for the method of description.

**Figure 3.** CCSD(T)/BLYP DDP BSEs (kcal/mol) except for 2,5-DDP, for which BD(T)/BLYP BSEs are plotted.

(the differential thermal contributions to the singlet and triplet spin states are, however, rarely more than 0.1 or 0.2 kcal/mol). Table 3 provides the 0 K S–T splittings for the 10 DDPs at each level of theory. Note that the correction of the BSEs implied by eqs 3 and 4 above is equivalent to computing the 0 K enthalpy change for the isodesmic reaction



and then adding to this the experimental value<sup>14,54</sup> for the S–T splitting of the relevant benzyne. We note again that this correction scheme dramatically reduces differences in predictions from different levels of theory (for specialists interested in the uncorrected performance of the various levels of theory, the raw data are provided as Supporting Information).

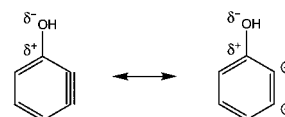
Also listed in Table 3 are S–T splittings predicted from a correlation of that quantity with BPW91/cc-pVDZ proton hyperfine coupling constants in appropriate antecedent radicals. Thus, for instance, the hfs for the proton at position 3 in the 2-dehydrophenol radical can be used to predict the S–T splitting in 2,3-DDP.<sup>25,27,35,55</sup> The raw S–T splittings predicted from the relevant correlations were corrected by the amount needed to bring the corresponding value predicted for the corresponding parent benzyne into agreement with experiment. The overall agreement between the hfs-predicted S–T splittings and those computed directly is impressive. This is especially true insofar as this method for prediction of the S–T splittings involves

(55) The correlating equation used for the *ortho* and *meta* radicals was (S–T splitting, kcal/mol) =  $-1.39 \times (^1\text{H hfs, G}) - 9.48$ , and that for the *para* radicals (S–T splitting, kcal/mol) =  $-1.99 \times (^1\text{H hfs, G}) - 0.30$ . The values in Table 3 are, where appropriate, averages over the two possible hfs values that can be used, e.g., the S–T splitting for 2,3-DDP is the average computed from using the hfs for position 3 in 2-dehydrophenol and for position 2 in 3-dehydrophenol.

only very economical DFT calculations for the three unique doublets, which do not suffer from any of the various technical challenges encountered for individual singlet and triplet DDP species.

**ortho Diradicals.** BSEs for the *ortho* singlets are predicted to be the most negative while those for the triplets are predicted to be the most positive over all the DDPs. This is entirely as expected insofar as the singlets have substantial triple bond character while the triplets suffer from enhanced exchange repulsion associated with the proximity of the two parallel spins. The identical situation is observed for the benzyne.<sup>14,56</sup>

More interestingly, the BSE for 2,3-DDP is predicted to be larger than that for 3,4-DDP at every level of theory. This effect does not appear to be hyperconjugation of the in-plane 2,3- $\pi$  bond into the parallel C–O  $\sigma^*$  orbital: the average C–O distance in the two rotamers of 2,3-DDP is 1.362 Å while in 3,4-DDP this value is 1.374 Å; if hyperconjugation into the C–O  $\sigma^*$  orbital were operative in 2,3-DDP one would expect the C–O bond to be longer, not shorter, than it is in 3,4-DDP. The difference seems to be the extent to which a zwitterionic mesomer contributes to the electronic structure of 2,3-DDP. The C–O bond dipole stabilizes development of anionic charge at the 2 position and cationic charge at the 3 position. In 3,4-DDP, interaction with the C–O bond dipole is much less effective.



Analysis of relevant bond angles supports this rationalization. These angles for the dehydro carbons in 2,3-DDP are somewhat unusual. In the *syn* isomer of 2,3-DDP (i.e., the hydroxyl proton is on the same side of the ring as the triple bond), the CCC bond angle at the 2 position is 118.6° while at the 3 position it is 135.7°. This contrasts significantly with the *syn* isomer of 3,4-DDP, where the bond angles at the 3 and 4 positions are 126.9° and 127.2°, respectively. The *anti* rotamers in each case have very similar bond angles to the *syn*. The distortion in the 2,3-case is consistent with carbanion development at the 2 position and carbocation development at the 3 position. Analysis of charge separation across the formal triple bond is further consistent with this rationalization. The CM2 charge of C(2) is 0.14 charge units more negative than C(3) in 2,3-DDP, while in 3,4-DDP the difference in charges between C(3) and C(4) is only 0.02 charge unit. All of the above effects are essentially absent in the *ortho* triplets, again supporting the contention that it is the degree of polarization of the in-plane  $\pi$  bond that differentiates 2,3- and 3,4-DDP.

Table 1 indicates that the polarization present in the 2,3-DDP singlet provides a BSE about 2 kcal/mol more negative than

(56) Cramer, C. J.; Nash, J. J.; Squires, R. R. *Chem. Phys. Lett.* **1997**, 277, 311.

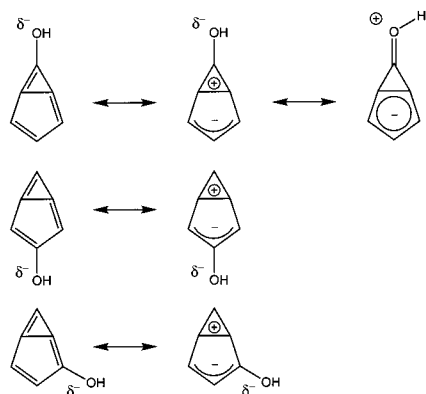


**Figure 4.** Resonance structures associated with bicyclic forms of the *meta* DDPs.

that for singlet *o*-benzyne,<sup>54</sup> while the BSE for triplet 2,3-DDP is predicted to be about 1 kcal/mol more *positive* than that for *o*-benzyne. Taken together, these lead to a S–T splitting for 2,3-DDP that is some 3 to 4 kcal/mol larger than that found for *o*-benzyne. These results are fairly insensitive to which hydroxyl rotamer is considered. The BSEs for 3,4-DDP, on the other hand, are quite close to those of *o*-benzyne, as is, necessarily, the S–T splitting—again there is little sensitivity to choice of hydroxyl rotamer. Thus, the perturbing effect of the hydroxyl group on the *o*-benzyne system is limited to the case where it is immediately adjacent to the formal triple bond.

***meta* Diradicals.** There are four *meta* DDPs: 2,6-, 3,5-, and two hydroxyl rotamers of 2,4-DDP. As the properties of 2,4-DDP show very little sensitivity to choice of hydroxyl rotamer, for ease of discussion below all quantitative values for 2,4-DDP will be taken from the *syn* rotamer.

Among the *meta* singlets, 2,6-DDP and 3,5-DDP have shorter interdehydrocarbon distances—1.988 and 1.978 Å, respectively—than does 2,4-DDP at 2.023 Å (cf. 2.021 Å for *m*-benzyne at the same level of theory). Thus, the 2,6 and 3,5 isomers may be regarded as being more highly distorted toward a bicyclic structure, and such a preference in these systems compared to 2,4-DDP can be understood by consideration of the polarization of the  $\pi$  system. As the aromatic ring distorts toward a hydroxyl-substituted bicyclo[3.1.0]hexa-1,3,5-triene, the bicyclic system can adopt some character of a zwitterionic resonance structure involving fusion of a formally aromatic cyclopropenium cation and an allyl anion (Figure 4). The contribution of this mesomer is manifest in the partial charges of the terminal allyl CH groups. In the limits of optimizing 2,6- and 3,5-DDP structures with constrained interdehydrocarbon distances of 2.4 and 1.4 Å, CM2 charges for these groups are about 0.08 electronic charge unit more negative in the bicyclic structures than in the monocyclic one.

The C–O bond lengths of the 2,6- and 3,5-DDPs, 1.362 and 1.368 Å, respectively, are also consistent with a significant contribution from the zwitterionic resonance structures invoked above. Both distances are shorter than the BLYP optimized C–O bond length in phenol, 1.381 Å, which is comparable to that predicted for 2,4-DDP, 1.385 Å. The interaction between the oxygen  $\pi$ -like lone pair and the cyclopropenium ion to which it is directly attached in 2,6-DDP is clearly stabilizing insofar as the system has the character of a protonated cyclopropenone (Figure 4). The stabilizing interaction between the oxygen lone pair and the allyl anion in 3,5-DDP is more subtle, and best discussed in conjunction with an analysis of the  $\pi$  system for 2,4-DDP.

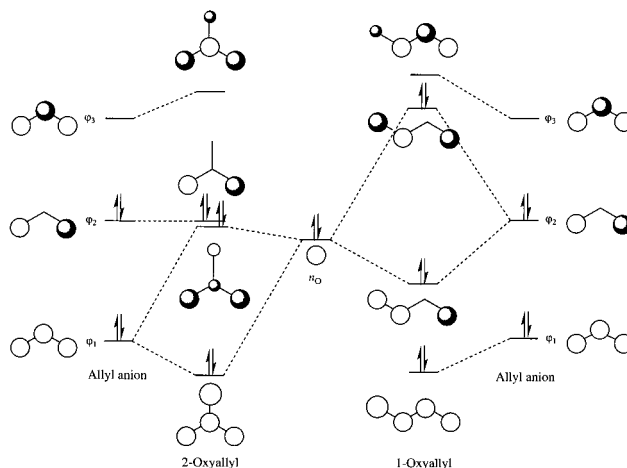


**Figure 5.** Mixing of allyl anion and nonbonding oxygen orbitals to form 2-oxyallyl (left) and 1-oxyallyl (right) MOs. Some mixing lines are left out for clarity.

We consider first the interaction of an allyl  $\pi$  system with a parallel oxygen lone pair substituted at position 2. Neglecting the small symmetry breaking effect of the hydroxyl proton, only allyl orbitals  $\phi_1$  and  $\phi_3$  are of the proper symmetry to mix with the oxygen lone pair (Figure 5), and the resulting orbitals are those of a heteroatomic trimethylenemethane (TMM) equivalent.<sup>57–68</sup> This mixing is weakly stabilizing for heteroatomic 6-electron system and thus favors distortion of 3,5-DDP toward a bicyclic structure (as probably does also inductive stabilization of the allyl anion by the substituting oxygen).

The longer C–O and interdehydrocarbon distances in the 2,4-DDPs, on the other hand, are due to a *destabilizing* interaction between the oxygen lone pair and the developing allyl anion in the zwitterionic resonance structure. If an allyl anion is perturbed with a lone pair that has significant overlap with  $\phi_2$ , then this 4-electron repulsive interaction dominates the orbital mixing (Figure 5) and the net effect is to mitigate against contraction toward a bicyclic structure.

The above analysis rationalizes the trend in singlet BSEs for the *meta* DDPs. The strongest resonance interaction involving the protonated cyclopropenone in singlet 2,6-DDP leads to a BSE that is about 6 kcal/mol more negative than that for singlet *m*-benzyne.<sup>54</sup> The somewhat weaker but still stabilizing interaction found in singlet 3,5-DDP leads to a BSE about 3 kcal/mol more negative. And, the *destabilizing* interaction noted for singlet 2,4-DDP is made manifest by a BSE about 2 kcal/mol *less* negative than that for *m*-benzyne. Kraka et al.<sup>23</sup> noted the destabilization present in the 2,4-DDP system by a somewhat different analysis, computing the 0 K enthalpy for the isodesmic reaction

- (57) Longuet-Higgins, H. C. *J. Chem. Phys.* **1950**, *18*, 265.
- (58) Dowd, P. *J. Am. Chem. Soc.* **1966**, *88*, 2587.
- (59) Borden, W. T.; Salem, L. S. *J. Am. Chem. Soc.* **1973**, *95*, 932.
- (60) Pople, J. A.; Seeger, U.; Seeger, R.; Schleyer, P. v. R. *J. Comput. Chem.* **1980**, *1*, 199.
- (61) Osamura, Y.; Borden, W. T.; Morokuma, K. *J. Am. Chem. Soc.* **1984**, *106*, 5112.
- (62) van de Guchte, W. J.; Zwart, J. P.; Mulder, J. J. C. *J. Mol. Struct. (THEOCHEM)* **1987**, *152*, 213.
- (63) Wiberg, K. B. *J. Am. Chem. Soc.* **1990**, *112*, 4177.
- (64) Coolidge, M. B.; Yamashita, K.; Morokuma, K.; Borden, W. T. *J. Am. Chem. Soc.* **1990**, *112*, 1751.
- (65) Gobbi, A.; MacDougall, P. J.; Frenking, G. *Angew. Chem., Int. Ed. Engl.* **1991**, *30*, 1001.
- (66) Skancke, A. *J. Phys. Chem.* **1994**, *98*, 5234.
- (67) Cramer, C. J.; Smith, B. A. *J. Phys. Chem.* **1996**, *100*, 9664.
- (68) Li, J.; Worthington, S. E.; Cramer, C. J. *J. Chem. Soc., Perkin Trans. 2* **1998**, 1045.



to be 3.4 kcal/mol at the B3LYP/6-31G\*\* level. Our own calculations for reaction 6 at the CCSD(T)//BLYP level yield a value of 3.5 kcal/mol. The positive sign for this enthalpy of reaction indicates the degree to which it is less favorable to substitute *m*-benzyne in the 4-position compared to benzene.

To within experimental error, the triplet BSEs for all *meta* DDP isomers are the same as that measured for *m*-benzyne.<sup>14,54</sup> Thus, the trend in S–T gaps for the *meta* DDPs directly reflects the degree of stabilization of the singlets (Figure 3).

***para* Diradicals.** As has been noted for other low-symmetry *p*-arynes,<sup>33–35,69</sup> the CCSD(T) method with a HF reference cannot be used for 2,5-DDP because very large singles amplitudes lead to instability in the estimation of the correlation energy associated with triple excitations. BD(T) calculations alleviate this instability.

Substitution of *p*-benzyne by a hydroxyl group is predicted to decrease the S–T splitting by about 2 kcal/mol. It is difficult to rationalize this decrease, however, as the singlet and triplet BSEs are predicted to agree with those for *p*-benzyne to well within the experimental error (the error for the *p*-benzyne BSEs is larger than that for its S–T splitting because the heats of formation required for eq 3 are measured to lower accuracy than are the S–T splittings derived from negative ion photoelectron spectroscopy<sup>14</sup>). Thus, it is not clear whether the smaller gap derives from singlet destabilization, triplet stabilization, or some combination of the two.

One possibility is that the empty C–O  $\sigma^*$  orbital in 2,5-DDP mixes slightly with the MO derived from symmetric combination of the two nonbonding orbitals. The latter MO is formally empty in the singlet state and singly occupied in the triplet,<sup>53,56</sup> so the interaction would be expected to favor the triplet and reduce the S–T splitting. Since experimental uncertainties do not allow us to be definitive, we have undertaken some additional calculations to explore this point, as well as to further bolster our analysis for *ortho* and *meta* isomers.

**Other Substituents.** Table 4 compares, for the CCSD(T) level using the isodesmic correction scheme embodied in eq 5, S–T splittings of the DDPs to those computed for the six possible didehydroanilines (DDAs) and didehydrobenzonitriles (DDBNs). Complete energetic and geometric results for these systems will be reported elsewhere.<sup>70</sup> The DDAs and DDBNs are not subject to rotational isomerism associated with the substituent group; to clarify substituent comparisons, the DDP values in Table 4 are averaged over both hydroxyl rotamers for the 2,3-, 2,4-, 2,5-, and 3,4-positional isomers.

We compare amino, hydroxyl, and cyano groups as substituents. To the extent we have invoked effects associated with donation of  $\pi$ -electron density, the amino group is the strongest  $\pi$ -donor, the hydroxyl group next strongest, and the cyano group is  $\pi$ -electron withdrawing; with respect to electronegativity/ $\sigma$ -electron withdrawing character, hydroxyl is the strongest inductive acceptor, amino is next strongest, and cyano is weakly accepting.<sup>71</sup>

Thus, for the 2,3-isomer, we have inferred an increased S–T splitting to be associated with bond-dipole-aligned stabilization of a zwitterionic singlet mesomer. Based on inductive power, this effect should be largest for hydroxyl, smallest for cyano, and intermediate for amino. This is indeed the trend observed in Table 4, with a total span of 3.2 kcal/mol. In the 3,5-isomer,

**Table 4.** Corrected CCSD(T)/cc-pVDZ//BLYP/cc-pVDZ S–T Splittings ( $H_0$ , kcal/mol) for Substituted Benzyne<sup>a</sup>

level	<i>ortho</i>		<i>meta</i>		<i>para</i>	
	2,3	3,4	2,6	3,5	2,4	2,5
DDA	–40.1	–37.0	–28.3	–23.8	–18.7	–2.4
DDP	–41.5	–36.0	–27.1	–24.2	–18.4	–1.9
DDBN	–38.3	–37.5	–21.3	–21.2	–20.6	–3.4

<sup>a</sup> See eqs 3–5 and discussion in text.

we have similarly proposed that the inclusion of a highly electronegative atom in a TMM-like system stabilizes a zwitterionic singlet mesomer and thereby increases the S–T splitting. Thus, the trend in this system should be the same as for the 2,3-isomer (OH > NH<sub>2</sub> > CN), and this is indeed what is observed, with the range of S–T splittings spanning 3.0 kcal/mol.

In the case of the 2,6-DDP isomer, we inferred  $\pi$ -donation to stabilize cyclopropenium cation character in a zwitterionic mesomer and thereby to increase the S–T splitting. As expected for this analysis, the magnitude of the splitting increases when the hydroxyl group is replaced by the better  $\pi$ -donating amino group and decreases when the replacing group is cyano. Table 4 indicates the range of the effect to be 7.0 kcal/mol, which is 33% of the prototypical *m*-benzyne S–T splitting. Similarly, we invoked a destabilizing interaction between terminal  $\pi$ -density in the allyl anion of a singlet mesomer and the hydroxyl group lone pair in rationalizing the lower than expected S–T splitting in 2,4-DDP. Consistent with this analysis, the singlet destabilization is about the same in the analogous DDA and reduced by 2.2 kcal/mol in the analogous DDBN, which has a  $\pi$ -electron-withdrawing group substituting the anionic position.

For the above isomers, effects on the S–T splitting were rationalized as deriving from differential effects on the singlet BSEs. While the data for the DDAs and DDBNs are not shown here, it is indeed the case that the majority of the differences in the S–T splittings as a function of substitution is attributable in every instance to changes in singlet BSEs, with only very small perturbations observed for triplet BSEs.

We return, last, to our speculation that in the 2,5-isomer an adjacent low-energy  $\sigma^*$  acceptor orbital may stabilize the triplet over the singlet (since the former has the occupied orbital of highest energy). As expected from such a prediction and the inductive power of the groups examined, Table 4 indicates the S–T splitting to be smallest (i.e., triplet most stabilized, albeit still above the singlet) for the DDP, next smallest for the DDA, and largest for the DDBN. In this case, it is the variation in the triplet BSEs that dominates the effect.

Thus, in every isomer, trends in chemical substitution are consistent with perturbation effects rationalized in the DDPs based on analysis of differences in geometries and electronic structures. Improved understanding of these interactions between substituent groups and arynes should prove useful in the design of systems having specifically targeted S–T splittings.

**Acknowledgment.** We thank the National Science Foundation, the Alfred P. Sloan and John Simon Guggenheim Foundations, the Spanish Ministry of Education and Culture, and Fundacion BBV for financial support, the Minnesota Supercomputer Institute for computational resources, and Professors Bob Squires and Hilkka Kenttämää for stimulating discussion.

**Supporting Information Available:** Optimized geometries and energies for the didehydrophenols, hydroxyphenyls, and phenol (PDF). This material is available free of charge via the Internet at <http://pubs.acs.org>.

JA002250L

(69) Schreiner, P. R.; Prall, M. J. *Am. Chem. Soc.* **1999**, *121*, 8615.

(70) Johnson, W. T. G.; Cramer, C. J. To be submitted for publication.

(71) March, J. *Advanced Organic Chemistry*, 4th ed.; John Wiley & Sons: New York, 1992; p 36.